
A Consciousness-Inspired Planning Agent for Model-Based Reinforcement Learning

Mingde Zhao^{1,4,*}, Zhen Liu^{2,4,*}, Sitao Luan^{1,4,*}, Shuyuan Zhang^{1,4,*}
Doina Precup^{1,3,4,†}, Yoshua Bengio^{2,4,†}
¹McGill University; ²Université de Montréal; ³DeepMind; ⁴Mila
*: Equal Contribution, †: Equal Supervision

Abstract

We present an end-to-end, model-based deep reinforcement learning agent which dynamically attends to relevant parts of its state, in order to plan and to generalize better out-of-distribution. The agent’s architecture uses a set representation and a bottleneck mechanism, forcing the number of entities to which the agent attends at each planning step to be small. In experiments with customized MiniGrid environments with different dynamics, we observe that the design allows agents to learn to plan effectively, by attending to the relevant objects, leading to better out-of-distribution generalization.

1 Introduction

Whether when planning our paths home from the office or from a hotel to an airport in an unfamiliar city, we typically focus our attention on a small subset of relevant variables, *e.g.* the change in position or the presence of obstacles on the planned path. It is plausible that this ability contributes to the ease with which humans handle novel situations. An interesting hypothesis is that this ability may be due to a style of computation associated with the conscious processing of information [2, 4, 3, 15]. Conscious attention focuses on a few necessary environment elements, with the help of an abstract representation of the world internal to the agent [45, 15]. This pattern, also known as consciousness in the first sense (C1) [15], has been theorized to be the source of humans’ exceptional ability to generalize or adapt well to new situations, and learn skills or new concepts efficiently from very few examples [2, 4, 3, 15, 45, 8, 17]. A central characteristic of conscious processing is that it involves a *bottleneck*, which forces one to handle dependencies between very few characteristics of the environment at a time [15, 8, 17]. Although this focus on a small subset of the available information may seem limiting, it may facilitate Out-Of-Distribution (OOD) and systematic generalization, *e.g.* to other settings where the ignored variables are different [8, 17].

In this paper, we propose an end-to-end architecture which allows us to encode some of these ideas into reinforcement learning agents. Reinforcement learning (RL) is a natural approach for combining learning how to act from interaction with a complex environment, and planning to achieve new goals [42]. However, most of the big successes of RL have been obtained by deep, model-free agents [31, 38, 39]. While Model-Based RL (MBRL) has generated significant research [32], its empirical performance has typically lagged behind, with the notable exception of MuZero [37]. We note that most MBRL agents work in the observation space, again with the exceptions of the Predictron [40] and MuZero [37, 21].

Our proposal is to use inspiration from human conscious planning to build an architecture which can learn a latent space useful for planning and in which attention can be focused on a small set of variables at any time. This builds on the idea of partial planning [43]

with modern deep RL architectures. More specifically, we build and train an end-to-end latent-space MBRL agent which does not require reconstructing the observations, and uses tree-search based Model Predictive Control (MPC) as the planning algorithm [35, 36, 49]. Our model uses a set-based representation to construct a latent state from its observations, and a selective attention bottleneck mechanism to plan over dynamically selected aspects of the state (Sec. 4). Our experiments show that these architectural constraints improve both sample complexity and OOD generalization, compared to more conventional MBRL methods (Sec. 5).

2 Background & Context

We consider an agent interacting with its environment at discrete time steps. At time t , the agent receives observation o_t and takes action a_t , receiving a reward r_{t+1} and new observation o_{t+1} . The interaction is episodic. The agent is also building a latent-space transition model, \mathcal{M} , which can be used to sample a next latent state, \hat{s}_{t+1} , a reward \hat{r}_{t+1} and a binary signal \hat{w}_{t+1} which indicates if the model predicts termination after the transition. We will now compare and contrast our approach with some existing methods from the MBRL literature, explaining the rationale for the choices we made.

Observation Level Planning and Reconstruction vs Latent Space Planning

Many MBRL methods plan in the observation space or rely on reconstruction-based losses to obtain state representations [16, 26]. These methods may be appropriate for some robotic tasks with few sensory inputs, *e.g.* continuous control with joint states, but they are arguably difficult with high-dimensional inputs like images [34], because they may focus on aspects of the raw observations that are not useful to the agent, yet which are predictable [32]. Besides suffering from the need to reconstruct noise or irrelevant parts of the signal, it is not clear if representations built by a reconstruction loss (*e.g.* L_2 in the observation space) are effective for an MBRL agent to plan and predict the desired signals [40], *e.g.* values (in the RL sense), rewards, *etc.*. In this work, we use an approach similar to the Predictron [40] and MuZero [37], building a latent representation that is jointly shaped by the relevant RL signals (to serve value estimation and planning) without using a reconstruction loss.

Staged Training vs End-to-End Training

Some MBRL agents based on a world model [18, 26, 32] use two explicit stages of training: (1) an inner representation of the world is trained using exploration (usually with random trajectories); (2) the representation is fixed and used for planning and MBRL. Despite the advantages of being more stable and easier to train, this procedure relies on having an environment where the initial exploration provides transitions that are sufficiently similar to those observed under improved policies, which is not the case in many environments. Furthermore, the learned representation may not be effective for value estimation, if these transitions do not contain reward information that can be used to update the input-to-representation encoder. End-to-end MBRL agents, *e.g.* [40, 37], are able to learn the representation online, simultaneously with the value function, hence adapting better to non-stationarity in the transition distribution and rewards.

Type of planning

MBRL agents can use the model in different ways. Dyna [41] learns a model to generate “imaginary” transitions, which contribute to the training of the value estimator [41, 49], in addition to the real observations, thus boosting sample efficiency. However, if the model is inaccurate, the transitions it generates may be “delusional”, which may alter the value function and negatively impact performance. Moreover, Dyna is typically used to generate extra transitions from the states visited in a trajectory, and updates the models based on the observed transitions as well, which means that it is focused on the data distribution encountered by the agent and may have trouble generalizing OOD. In contrast, simulation-based model-predictive control (MPC) and its variants [35, 36, 49] only update the value function based on real data, using the model simply to perform lookahead. Hence, model inaccuracies have less impact. OOD generalization can also be favorable, depending on the losses and model class chosen. Hence, we use MPC in our approach.

Vectorized vs Set Representations for RL

Most existing Deep Reinforcement Learning (DRL) work is based on vectorized representations, in which the agent’s observation is transformed into a feature vector of fixed size [31, 19].

Instead, set-based encoders, *a.k.a.* object-oriented architectures, are designed to extract a set of unordered vectors from which to predict the desired signals via permutation-invariant computations [53], as illustrated in Fig. 1. Recent works on representation learning for RL have shown the promise of set-based representations in capturing dynamics, in terms of generalization, as well as their similarities to human perception [14, 50, 33, 48, 30]. Apart from these motivations, in this work, we utilize the compositionality of set representations to enable the discovery of sparse interactions among objects, *i.e.* learning underlying dynamics, as well as to facilitate the bottleneck mechanism, analogous to C1 selection. The set-based representation coupled with the workspace bottleneck provides an inductive bias consistent with selecting only the relevant aspects of a situation on-the-fly through an attention mechanism, with different aspects considered depending on the task. We expect this to yield better OOD generalization, because of the interchangeability of the objects arising from the permutation-invariance of these computations and because many aspects will be ignored by the bottleneck, and therefore can change without disrupting the plan. The small size of the working memory bottleneck also enforces sparsity of the dependencies [8, 17] captured by the learned dynamics model: each transition can only relate a few objects together, no more than the size of the bottleneck.

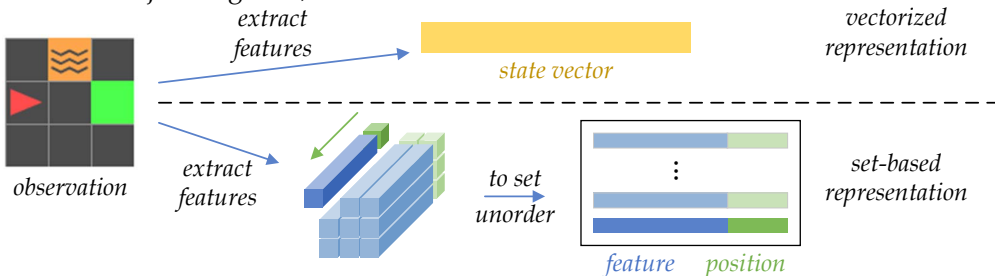


Figure 1: **Set-based state encoder** compared to classical vectorized state encoders: the feature map extracted by some feature extractor, *e.g.* CNN, is “chopped” into feature vectors and concatenated with positional information. All of the resulting concatenations are treated as *objects* in a set, capturing the features of observed entities. The permutation-invariance of set computations forces the learner to be robust to small changes in the set (*e.g.* one of the elements being different or missing).

3 MBRL with Set Representations

In this section, we present an end-to-end baseline MBRL agent that uses a set-based representation and carries out latent space planning, but **without** having a small bottleneck. This serves as the basis of the proposed planning agent introduced in Sec. 4.

The mapping from observations to values is a combination of an *encoder* and a *value estimator*. The encoder maps an observation vector to a set of objects, which constitutes the latent state. The value estimator is a permutation-invariant set-to-vector architecture that maps the latent state to a value estimate. Note that the same latent state is used for all the agents’ predictions, including future states, rewards *etc.*, as we will discuss later.

Encoder. We use the features at each position of the output feature map of a CNN to characterize an object, similar to [10]. To preserve positional information when interpreting these vectors as an unordered set, we concatenate each of them with a positional embedding. This approach is different from the practice of adding positional information onto the features [10, 47], and we adopt it for the compatibility with our procedure for training the dynamics model, discussed below.

(State-Action) Value Estimator takes the form $Q : \mathcal{S} \rightarrow \mathbb{R}^{|\mathcal{A}|}$, where \mathcal{S} is the latent state space (of sets) constructed by the encoder and \mathcal{A} is a discrete action set. We use an adapted version of the DeepSets architecture [53], depicted in Figure 2.

Transition Model. The transition model maps from s_t, a_t to \hat{s}_{t+1}, \hat{r}_t and $\hat{\omega}_{t+1}$. We separate this into: 1) the **dynamics model**, in charge of simulating how the state would change with the input of s_t, a_t and 2) the **reward-termination estimator** which maps s_t, a_t to \hat{r}_t and $\hat{\omega}_{t+1}$.

While the design of the reward-termination estimator is straightforward (a two-headed augmented architecture similar to the value estimator), the dynamics model requires

regression on *unordered* sets of objects (set-to-set). A common approach is to use matching-based losses, *e.g.* Chamfer matching or Hausdorff distance, but they are computationally demanding and subject to local optima [6, 9, 29]. Luckily, our feature-position separated set encoding method not only makes the permutation-invariant computations position-aware, but also allows simple end-to-end training over the dynamics. By forcing the positional tails to be immutable during the computational pass, we can use them to solve the matching trivially: objects “labeled” with the same positional tail in the prediction \hat{s}_{t+1} (output of the dynamics model) and the training sample s_{t+1} (state obtained from the next observation) are aligned, forming pairs of objects with changes *only* in the feature, as shown in Figure 3.

Tree Search MPC. The model-based agent employs a tree-search based behavior policy (with ϵ -greedy exploration). During planning, each tree search call maintains a priority queue of promising branches to simulate with the model *s.t.* the most promising path could be selected. When a designated budget (*e.g.* number of steps of simulation) is spent, the agent greedily picks the immediate action that leads to the most promising path. We present the pseudocode of the Q-value based prioritized tree-search MPC in Appendix.

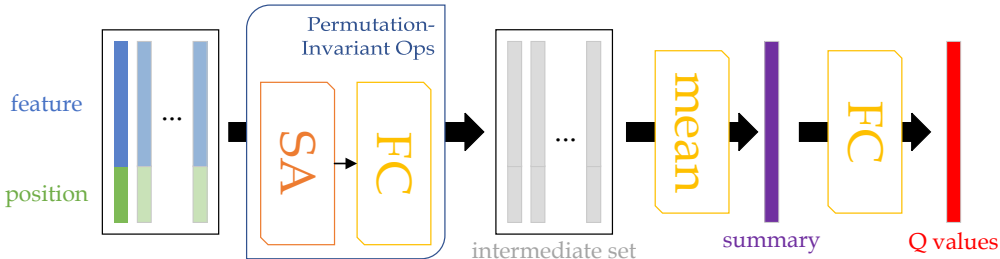


Figure 2: **Value estimator Q and a generic set-to-vector architecture:** we modify the design of DeepSets [53] by replacing the MLP before pooling with transformer layers (multi-head Self-Attention (SA) + object-wise Fully Connected (FC)) [47]. We found this change to be helpful for the learning performance. After applying the transformer layers, the intermediate set (colored gray) entangles features and positions. Please check the Appendix for more details on the self-attention operations involved.

For training and in-distribution evaluation, the tree search employs a best-first search heuristic: the search is directed to the branches that are most promising according to the value estimator. For OOD evaluation, we found the value estimator to be insufficiently reliable to guide the search and hence we use random branching instead.

Compared to Monte-Carlo Tree Search (MCTS) [38, 39], this method traces the branches at shallower depths during expansion, yet it can flexibly branch the search tree at different depth levels. The method is compatible with deterministic policies *w.r.t.* the estimator parameters and requires significantly fewer simulations (see example in Appendix).

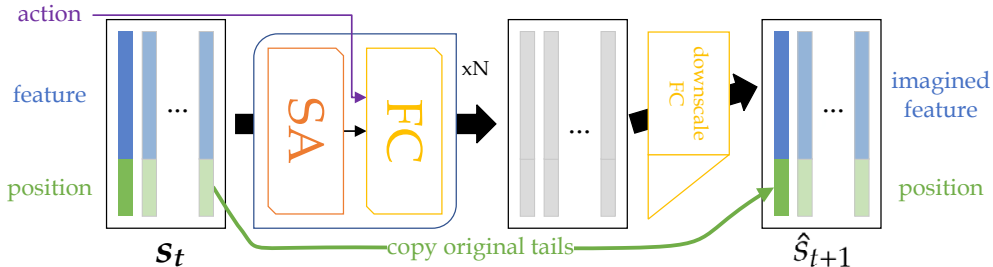


Figure 3: **Dynamics model (state simulation operator):** for FC sub-layers of the transformer layers, we inject an additional action embedding *s.t.* the transformer set-to-set computations are action conditioned. After getting the intermediate set, we downscale each of the objects to the imagined features, leaving the positions untouched and directly copied from the input s_t . Intuitively, we make each object “memorize” its positional tail during the transformation and recover it at the output. Though the objects in the sets (input-intermediate-output) are aligned, within each set they are still unordered, *i.e.* the computation flow remains permutation-invariant.

Training. The proposed agent is trained from sampled transitions with the following losses:

- Temporal Difference (TD) \mathcal{L}_{TD} : regresses the current state value estimate to the update target, *e.g.* provided by DQN or Double DQN (DDQN) [31, 46]. In experiments, a distributional output is used for both value and reward estimation, making this loss a KL-divergence.
- Dynamics Consistency \mathcal{L}_{dyn} : A squared L_2 distance established between the aligned \hat{s}_{t+1} and s_{t+1} , where \hat{s}_{t+1} is the imagined next (latent) state given o_t, a_t and s_{t+1} is the true next (latent) state encoded from o_{t+1} .
- Reward Estimation \mathcal{L}_r : the KL-divergence between the imagined reward \hat{r}_{t+1} predicted by the model and the true reward r_{t+1} of the observed transition.
- Termination Estimation \mathcal{L}_ω : the binary cross-entropy loss from the imagined termination $\hat{\omega}_{t+1}$ to the ground truth ω_{t+1} , obtained from environment feedback.

The resulting total loss for end-to-end training of this set-based MBRL agent is thus:

$$\mathcal{L} = \mathcal{L}_{\text{TD}} + \mathcal{L}_{\text{dyn}} + \mathcal{L}_r + \mathcal{L}_\omega$$

Jointly shaping the state representation avoids the representation collapsing to trivial solutions and makes it useful for all signal predictions of interest. In our current implementation, no recurrent mechanism is included; however the same training procedure is naturally extendable to RNNs.

4 Using a Bottleneck

To enable better generalization, we introduce an inductive bias which aims to mimic a C1-like ability in the planning agent. In a nutshell, the planning is expected to focus on the parts of the world that matter for the plan. Simulations and predictions are all expected to be performed on a (small) bottleneck set, which contains all the important transition-related information. As illustrated in Figure 4, the model performs 1) selection of the bottleneck set from the full state-set, 2) dynamics simulation on the bottleneck set and 3) integration of predicted bottleneck set to form the predicted next state.

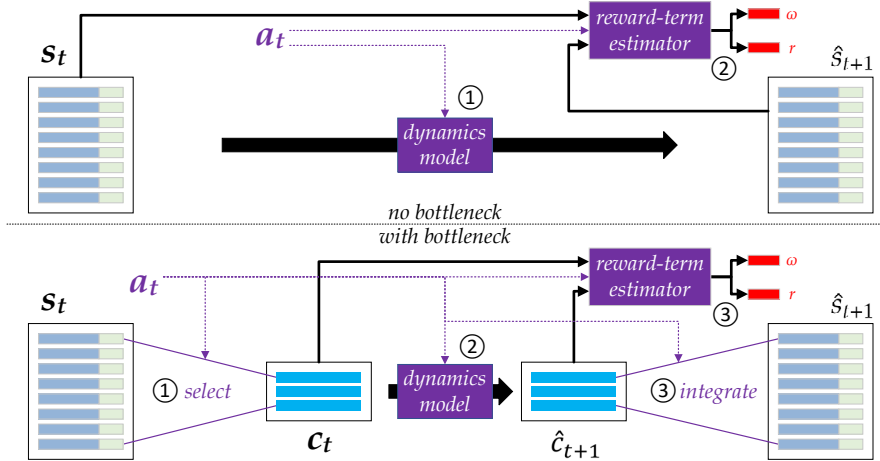


Figure 4: **Bottleneck stages** (operations colored in purple are conditioned on a chosen action): 1) a bottleneck set c_t is soft-selected from the whole state (object set) s_t through semi-hard multi-head attention; 2) dynamics are applied to the bottleneck set c_t to form \hat{c}_{t+1} ; 3) the reward and termination signals are predicted from c_t, \hat{c}_{t+1} and a_t . Then, the changes introduced in \hat{c}_{t+1} are integrated with s_t to obtain \hat{s}_{t+1} , the imagined next state, with the help of attention. Note that the two computational flows in stage 3 are naturally parallelizable.

Conditional State Selection We select a bottleneck set c_t of n objects (or memory slots) from the potentially large state set s_t of $m \gg n$ objects, and then only model the transition for the selected objects. To make this selection, we use a key-query-value attention mechanism, where the key and the value for each object in s_t are obtained from that object, and the query is a function of some learned dedicated set of vectors and of the action considered (see Appendix for details). Inspired by previous work on self-attention for memory access [27], we use a semi-hard top- k attention mechanism to facilitate the selection of the bottleneck

set. That is, after the query, the top- k attention weights are kept, all others are set to 0, and then the attention weights are renormalized. This semi-hard attention technique limits the influence of the ill-matched objects on the bottleneck set c_t while allowing for a gradient to propagate on the assignment of relative weight to different objects. With purely soft attention, weights for irrelevant objects are never 0 and learning to disentangle objects is more difficult in our experience.

Dynamics / Reward-Termination Prediction on Bottleneck Sets. We use the same reward-termination estimator architecture as described in Sec. 3, but taking the bottleneck objects as input rather than the full state. Details of the architecture are in the Appendix.

Change Integration. An integration operation is implemented to ‘soft paste-back’ the changes of the bottleneck state onto the state set s_t , yielding the imagined next state set \hat{s}_{t+1} . This is also achieved by attention operations, more specifically querying \hat{c}_{t+1} with s_t , conditioned on the action a_t . Please check the Appendix for details of the attention-related operations.

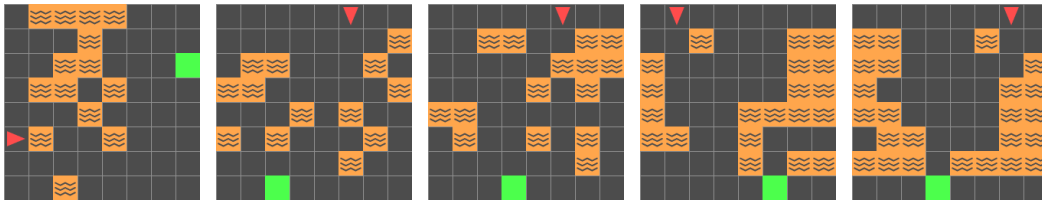
Discussion. The bottleneck that we described in this section is a natural complement to the MBRL model with set representations discussed previously. In particular, planning and training are carried out the same way as discussed in Sec. 3.

We expect the Conscious Planning (CP) agent to demonstrate the following advantages:

- **Higher Quality Representation:** the interplay between the set representation and the selection / integration forces the representation to be more disentangled and more capable of capturing the locally sparse dynamics.
- **More Effective Generalization:** only essential objects for the purpose of planning participate in the transition, thus generalization should be improved both in-distribution and OOD, because the transition does not depend on the parts of the state ignored by the bottleneck.
- **Lower Computational Complexity:** directly employing transformers to simulate the full state dynamics results in a computational complexity of $O(|s_t|^2d)$, where d is the length of the objects, due to the use of Self-Attention (SA), while the bottleneck lowers it to $O(|s_t||c_t|d)$.

5 Experiments

We describe a comprehensive set of experiments and ablation studies of our CP agent against baselines to assess in-distribution and OOD generalization, as well as planning performance.



(a) In-dist, diff 0.35 (b) OOD, diff 0.25 (c) OOD, diff 0.35 (d) OOD, diff 0.45 (e) OOD, diff 0.55

Figure 5: Non-Static RL Setting, with in-distribution and OOD tasks: (a) example of training environments (b - e) examples of OOD environments (rotated 90 degrees, changing the distribution of grid elements). For OOD testing, we evaluate different levels of difficulty (b - e). The agent (red triangle) points in the forward movement direction. The goal is marked in green. For each episode (training or OOD), we randomly generate a new world from a sampling distribution. Note that the training environments and the OOD testing environments have no intersecting observations.

5.1 Environment / Task Description

For the purposes of the experiments, we use environments based on the MiniGrid-BabyAI framework [12, 11, 22], which can be customized to require OOD generalization and to vary the difficulty of the planning task. In order to make sure we assess the agents as well as possible, the customized gridworld environments we designed feature clear object definitions, with well-understood underlying dynamics based on object interaction.

Furthermore, the environments are solvable by Dynamic Programming (DP) and can be easily tuned to generate OOD evaluation tasks. These characteristics are crucial for the experimental insights we are seeking.

The experiments are carried out on 8×8 gridworlds¹, as shown in Figure 5. The agent (red triangle) needs to navigate (by turning left, turning right or stepping forward) to the goal while dodging the lava grid cells along the way². If the agent steps into lava (orange square), the episode terminates immediately with no reward. If the agent successfully reaches the goal (green square), it receives a positive reward of +1 and the episode terminates. The discount factor is $\gamma = 0.99$. For better generalization, the agent needs to understand how to avoid lava in general (and not at specific locations, since their placement changes) and to reach the goal as quickly as possible. The environments provide grid-based observations that are ready to be interpreted as set representations: each pixel of any observation in the gridworld is an object, thus resulting in a set of 64 objects in s_t for each observation.

For the agent to be able to *understand* the environment dynamics instead of *memorizing* them³, we generate a new environment for each training or evaluation episode, which can be viewed as domain randomization [44]. In each training episode, the agent starts at a random position on the leftmost or rightmost edge and the goal is placed randomly somewhere along the opposite edge. In between the two edges, the lava squares are randomly generated according to a difficulty parameter which controls the independent probability of placing lava at a given grid position. The difficulty of the training episodes is fixed to 0.35.

For OOD evaluation, the agent is expected to adapt to the new environments with the same underlying dynamics in a 0-shot fashion, *i.e.* the agent’s parameters are fixed and no longer update. The OOD setting is crafted to change both the support (layout) and the distribution (difficulty) of the environment generation: the agent is deployed in *transposed* environments⁴ with varying levels of difficulty ($\{0.25, 0.35, 0.45, 0.55\}$). The differences of in-distribution (training) and OOD (evaluation) environments are illustrated in Figure 5.

We note that most usual RL benchmarks contain fixed environments, where the agent is expected to acquire a specific optimal policy. These environments are ill-suited for our purpose, since existing RL methods are known to be able to memorize such static environments well. Our experimental setup is too complex to allow memorization.

5.2 Agent Setting

We build all the set-based MBRL agents included in the evaluation on a common model-free baseline: a set-based variant of Double-DQN (DDQN) [46] with prioritized replay and distributional outputs. For more details, please check the Appendix.

We compare the proposed approach, labelled CP in the figures (for Conscious Planning) against the following methods:

- *UP* (for Unconscious Planning): the agent proposed in Section 3, lacking the bottleneck.
- *model-free*: the model-free set-based agent is the basis for both the CP and UP agents. It contains only the encoder and the value estimator, using the same architectures as in CP and UP.
- *Dyna*: the set-based MBRL agent which includes a model-free agent and an observation-level transition model, *i.e.* a transition generator. For the model, we use the CP transition model (with the same hyperparameters as the best performing CP agent) on the original environment features without an encoder. We also use the same hyperparameters as in the CP model training. The agent essentially doubles the batch size of the model-free baseline by augmenting training batches with an equal number of generated transitions.

¹Note that we did not use larger gridworlds because they would require more sophisticated exploration, which is not the focus of this work.

²In the Appendix, we provide an additional test setting with different dynamics for navigation, which also demonstrates the agents’ ability to work well despite cluttering distractions.

³This intuition has been validated in [52].

⁴the agent starts at the top or bottom edge and the goal is respectively on the bottom or top edge, whereas the training environment has the agent and goal on the left or right edges

- *Dyna**: A Dyna baseline that uses the true environment model for transition generation. This baseline is expected to demonstrate Dyna’s performance limit, assuming that the model works in observation space.
- *WM-CP*: A world model CP variant that differs from CP by following a 2-stage training procedure [18]. First, the model (together with the encoder) is trained with 10^6 random transitions. After this, the encoder and the model are fixed and RL begins.
- *NOSET*: A UP-counterpart with vectorized representations and no bottleneck mechanism.

Particularly, for CP and UP agents, we also test the following variants:

- *CP-noplan*: A CP agent that trains normally but does not plan in OOD evaluations, *i.e.* carrying out model-free behavior. This baseline aims to demonstrate the impact of planning in the training process on the OOD capability of the value estimator.
- *UP-noplan*: UP counterpart of CP-noplan.

Note that the compared methods share architectures as much as possible to ensure fair comparisons. More details of the compared methods, their architecture design and hyper-parameters are provided in the Appendix.

5.3 In-Distribution Evaluation

In Figure 6, we present the in-distribution evaluation curves for the different agents. For UP, CP and the corresponding model-free baselines, the performance curves show no significant difference, which demonstrates that these agents are effective in learning to solve the in-distribution tasks. During the “warm-up” period of the WM baseline, the model learns a representation that captures the underlying dynamics. After the warm-up, the encoder and the model parameters are fixed and only the value estimator learns to predict the state-action values based on the given representation. The increase in performance is not only delayed due to the warm-up phase (during which rewards are not taken into account) but also harmed, presumably because the value estimator has no ability to shape the representation to better suit its needs. The Dyna baseline performs badly while the Dyna* baselines perform relatively well. This is likely due to the delusional transitions generated by the model at the early stages of training, from which the value estimator never recovers. However, the Dyna* baseline does not achieve satisfactory OOD performance (Figure 7), presumably because its planning only focuses on observed data, and hence only improves the in-distribution performance, due to insufficiently strong generalization. The NOSET baseline performs very badly even in-distribution, per Figure 6. In the Appendix, we show that the NOSET baseline seems only able to perform well in a more classical, static RL setting, which may indicate that it relies on memorization. We provide more results regarding the model accuracy in the Appendix.

5.4 OOD Evaluation

The OOD evaluation focuses on testing the agents’ performance in a set of environments forming a gradient of task difficulty.

5.4.1 Task-Solving Performance

In Figure 7, we present the performance curves of the compared methods under different levels of OOD difficulty. CP(8), the CP agent with bottleneck size $n = 8$, shows a clear performance advantage over UP, validating its OOD generalization capability. The Dyna* baseline, essentially the performance upper bound of Dyna-based planning methods, shows no significant performance gain in OOD tests compared to model-free methods. WM may have the potential to reach similar performance as CP, yet it needs to warm up the encoder with a large portion of the agent-environment interaction budget.

5.4.2 Ablation

We validate design choices via ablation tests. Figure 8 visualizes two of these experiments. For more ablation results, which include validation of the effectiveness of different model choices, and further quantitative measurements, *e.g.* of OOD ability as a function of behavior optimality and model accuracy, please check the Appendix.

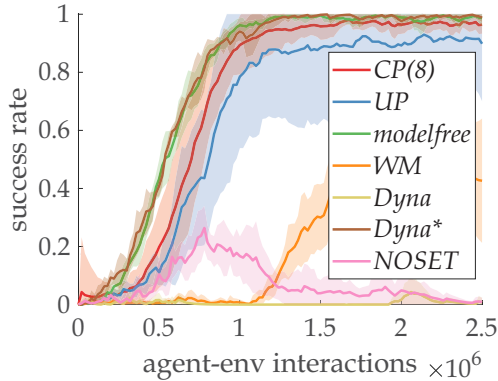
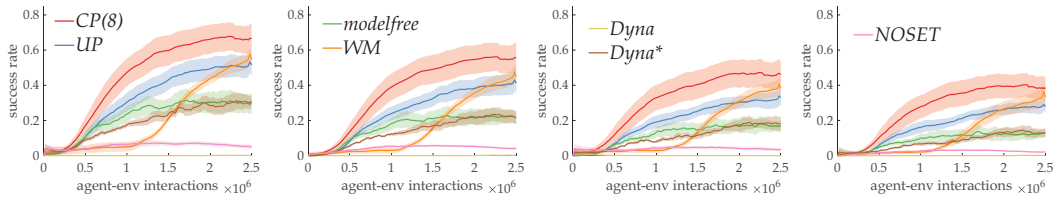
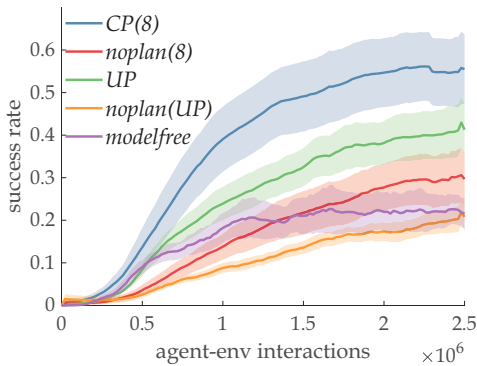


Figure 6: **In-distribution task performance:** the x -axis shows the training progress (number of actions executed, 2.5×10^6 agent-environment interactions). The y -axis values are generated by agent snapshots at times corresponding to the x -axis values. Each band shows the mean curve (bold) and the standard deviation interval (shaded) obtained from at least 5 independent runs. For each run, each data point used to obtain the bands is the average of 20 independent evaluations on newly generated environments. We adopt this curve collection method throughout the paper. CP, UP, model-free and Dyna* agents all learn to solve the in-distribution tasks quickly.

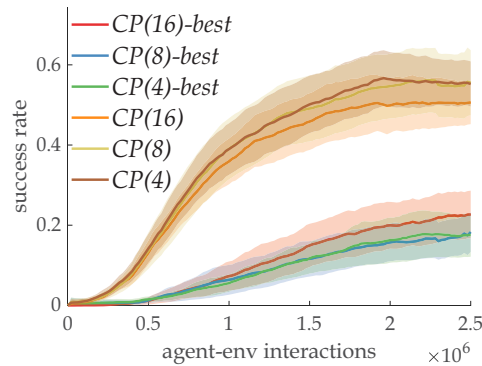


(a) OOD, difficulty 0.25 (b) OOD, difficulty 0.35 (c) OOD, difficulty 0.45 (d) OOD, difficulty 0.55

Figure 7: **OOD performance under different levels of difficulty.** These figures show a consistent pattern: the MPC-based end-to-end agent equipped with a bottleneck performs the best. The data for each figure is obtained through the procedure described above.



(a) **Bottleneck provides OOD capability:** noplan(8) and noplan(UP) correspond to the CP(8) and UP variants with planning disabled during OOD testing. Comparing the noplan baselines against the model-free, we see that planning during training is beneficial for both value estimation and state representation.



(b) **Value estimators are not expected to generalize well OOD:** random heuristic significantly outperforms best-first heuristic OOD.

Figure 8: **Key ablation results:** with difficulty 0.35, each band consists of the mean curve and standard deviation interval shades obtained from at least 5 independent runs.

5.5 Summary

The experiments allow us to draw the following conclusions:

- Set-based representations enable to generalization across different environment dynamics in multi-task or non-static environments, which force the learner to discover dynamics that are preserved across environments;
- Model-free methods face difficulties in OOD generalization;
- MPC-based planning exhibits better OOD generalization than Dyna-style algorithms;
- Online joint training of the representation with all the relevant signals is beneficial in RL, as suggested in [23];
- In accordance with our intuition, transition models with bottlenecks learn dynamics better, likely because they prioritize learning the aspects most relevant, while models without bottleneck have to waste capacity on irrelevant aspects. From further experiments provided in the Appendix, we observe that bottleneck-equipped agents are also less affected by cluttering, due to their prioritized learning of interesting entities.

6 Conclusion & Limitations

We introduced a conscious bottleneck mechanism into MBRL, facilitated by set-based representations, end-to-end learning and tree search MPC. In non-static RL settings, the bottleneck allows selecting the relevant objects for planning and hence enables significant OOD generalization in the CP agent, compared to more traditional baselines.

One limitation of our work is the experimental focus on only Minigrid environments, due to the need to validate carefully our approach. We would also like to extend these ideas to temporally extended models, which could simplify the planning task, and are also better suited as a conceptual model of C1. Finally, we note that the architectures we use are involved and can require careful hyperparameter optimization for new types of environments.

Acknowledgements

Mingde is grateful for the financial support from the Fonds de Recherche du Québec - Nature et Technologies (FRQNT). The authors are thankful for the helpful discussions with Xiru Zhu (about the design of the environment generation procedure), David Yu-Tung Hui (about the bag-of-word representations, the insights on BabyAI as well as helpful discussions about writing of the introduction section), Min Lin (about the design of the dynamics model as well as the early stage brainstorming) and Ian Porada (for the consistent support of the project).

References

- [1] J. L. Ba, J. R. Kiros, and G. E. Hinton. Layer normalization. *arXiv*, abs/1607.06450, 2016. <http://arxiv.org/abs/1607.06450>.
- [2] B. J. Baars. *A cognitive theory of consciousness*. Cambridge University Press, 1993.
- [3] B. J. Baars. The conscious access hypothesis: origins and recent evidence. *Trends in cognitive sciences*, 6(1):47–52, 2002.
- [4] B. J. Baars et al. *In the theater of consciousness: The workspace of the mind*. Oxford University Press, USA, 1997.
- [5] D. Bahdanau, K. Cho, and Y. Bengio. Neural machine translation by jointly learning to align and translate. *arXiv*, abs/1409.0473, 2014. <https://arxiv.org/abs/1409.0473>.
- [6] H. G. Barrow, J. M. Tenenbaum, R. C. Bolles, and H. C. Wolf. Parametric correspondence and Chamfer matching: 2 new techniques for image matching. Technical report, SRI International Menlo Park CA Artificial Intelligence Center, 1977.
- [7] M. G. Bellemare, W. Dabney, and R. Munos. A distributional perspective on reinforcement learning. *International Conference on Machine Learning*, 2017.
- [8] Y. Bengio. The consciousness prior. *arXiv*, abs/1709.08568, 2017. <http://arxiv.org/abs/1709.08568>.
- [9] G. Borgefors. Hierarchical chamfer matching: A parametric edge matching algorithm. *IEEE Transactions on pattern analysis and machine intelligence*, 10(6):849–865, 1988.
- [10] N. Carion, F. Massa, G. Synnaeve, N. Usunier, A. Kirillov, and S. Zagoruyko. End-to-end object detection with transformers. *European Conference on Computer Vision*, 2020. <https://arxiv.org/abs/2005.12872>.
- [11] M. Chevalier-Boisvert, D. Bahdanau, S. Lahlou, L. Willems, C. Saharia, T. H. Nguyen, and Y. Bengio. Babyai: A platform to study the sample efficiency of grounded language learning. *International Conference on Learning Representations*, 2018. <http://arxiv.org/abs/1810.08272>.
- [12] M. Chevalier-Boisvert, L. Willems, and S. Pal. Minimalistic gridworld environment for openai gym. *GitHub repository*, 2018. <https://github.com/maximecb/gym-minigrad>.
- [13] R. C. Conant and W. Ross Ashby. Every good regulator of a system must be a model of that system. *International journal of systems science*, 1(2):89–97, 1970.
- [14] G. Davidson and B. M. Lake. Investigating simple object representations in model-free deep reinforcement learning. *arXiv*, abs/2002.06703, 2020. <https://arxiv.org/abs/2002.06703>.
- [15] S. Dehaene, H. Lau, and S. Kouider. What is consciousness, and could machines have it? *Science*, 358, 2020. <https://science.sciencemag.org/content/358/6362/486>.
- [16] F. Ebert, C. Finn, S. Dasari, A. Xie, A. X. Lee, and S. Levine. Visual foresight: Model-based deep reinforcement learning for vision-based robotic control. *arXiv*, abs/1812.00568, 2018. <http://arxiv.org/abs/1812.00568>.
- [17] A. Goyal and Y. Bengio. Inductive biases for deep learning of higher-level cognition. *arXiv*, abs/2011.15091, 2020. <https://arxiv.org/abs/2011.15091>.
- [18] D. Ha and J. Schmidhuber. World models. *arXiv*, abs/1803.10122, 2018. <http://arxiv.org/abs/1803.10122>.
- [19] M. Hessel, J. Modayil, H. van Hasselt, T. Schaul, G. Ostrovski, W. Dabney, D. Horgan, B. Piot, M. G. Azar, and D. Silver. Rainbow: Combining improvements in deep reinforcement learning. *AAAI Conference on Artificial Intelligence*, 2017. <http://arxiv.org/abs/1710.02298>.
- [20] D. Horgan, J. Quan, D. Budden, G. Barth-Maron, M. Hessel, H. van Hasselt, and D. Silver. Distributed prioritized experience replay. *International Conference on Learning Representations*, 2018. <http://arxiv.org/abs/1803.00933>.
- [21] T. Hubert, J. Schrittwieser, I. Antonoglou, M. Barekatin, S. Schmitt, and D. Silver. Learning and planning in complex action spaces. *International Conference on Machine Learning*, 2021.

- [22] D. Y.-T. Hui, M. Chevalier-Boisvert, D. Bahdanau, and Y. Bengio. Babyai 1.1. *arXiv*, abs/2007.12770, 2020. <http://arxiv.org/abs/2007.12770>.
- [23] M. Jaderberg, V. Mnih, W. M. Czarnecki, T. Schaul, J. Z. Leibo, D. Silver, and K. Kavukcuoglu. Reinforcement learning with unsupervised auxiliary tasks. *International Conference on Representation Learning*, 2017.
- [24] M. Janner, J. Fu, M. Zhang, and S. Levine. When to trust your model: Model-based policy optimization. *arXiv*, abs/1906.08253, 2019. <http://arxiv.org/abs/1906.08253>.
- [25] N. Jiang, A. Kulesza, S. Singh, and R. Lewis. The dependence of effective planning horizon on model accuracy. In *Proceedings of the 2015 International Conference on Autonomous Agents and Multiagent Systems*, pages 1181–1189. Citeseer, 2015.
- [26] L. Kaiser, M. Babaeizadeh, P. Milos, B. Osinski, R. H. Campbell, K. Czechowski, D. Erhan, C. Finn, P. Kozakowski, S. Levine, et al. Model-based reinforcement learning for atari. *arXiv*, abs/1903.00374, 2019. <http://arxiv.org/abs/1903.00374>.
- [27] N. R. Ke, A. Goyal, O. Bilaniuk, J. Binas, M. C. Mozer, C. Pal, and Y. Bengio. Sparse attentive backtracking: Temporal credit assignment through reminding. *arXiv*, abs/1809.03702, 2018. <http://arxiv.org/abs/1809.03702>.
- [28] D. P. Kingma and J. Ba. Adam: A method for stochastic optimization. *International Conference on Learning Representations*, 2014. <http://arxiv.org/abs/1412.6980>.
- [29] A. R. Kosiorek, H. Kim, and D. J. Rezende. Conditional set generation with transformers. *arXiv*, abs/2006.16841, 2020. <http://arxiv.org/abs/2006.16841>.
- [30] S. Löwe, K. Greff, R. Jonschkowski, A. Dosovitskiy, and T. Kipf. Learning object-centric video models by contrasting sets. *CoRR*, 2011.10287, 2020.
- [31] V. Mnih, K. Kavukcuoglu, D. Silver, A. A. Rusu, J. Veness, M. G. Bellemare, A. Graves, M. Riedmiller, A. K. Fidjeland, G. Ostrovski, et al. Human-level control through deep reinforcement learning. *nature*, 518(7540):529–533, 2015.
- [32] T. M. Moerland, J. Broekens, and C. M. Jonker. Model-based reinforcement learning: A survey. *arXiv*, abs/2006.16712, 2020. <http://arxiv.org/abs/2006.16712>.
- [33] T. Mu, J. Gu, Z. Jia, H. Tang, and H. Su. Refactoring policy for compositional generalizability using self-supervised object proposals. *Advances in Neural Information Processing Systems*, 33, 2020.
- [34] A. S. Polydoros and L. Nalpantidis. Survey of model-based reinforcement learning: Applications on robotics. *Journal of Intelligent & Robotic Systems*, 86(2):153–173, 2017.
- [35] A. V. Rao. A survey of numerical methods for optimal control. *Advances in the Astronautical Sciences*, 135(1):497–528, 2009.
- [36] A. G. Richards. *Robust constrained model predictive control*. PhD thesis, Massachusetts Institute of Technology, 2005.
- [37] J. Schrittwieser, I. Antonoglou, T. Hubert, K. Simonyan, L. Sifre, S. Schmitt, A. Guez, E. Lockhart, D. Hassabis, T. Graepel, et al. Mastering Atari, Go, Chess and Shogi by planning with a learned model. *Nature*, 588(7839):604–609, 2020.
- [38] D. Silver, A. Huang, C. J. Maddison, A. Guez, L. Sifre, G. Van Den Driessche, J. Schrittwieser, I. Antonoglou, V. Panneershelvam, M. Lanctot, et al. Mastering the game of go with deep neural networks and tree search. *Nature*, 529(7587):484–489, 2016.
- [39] D. Silver, J. Schrittwieser, K. Simonyan, I. Antonoglou, A. Huang, A. Guez, T. Hubert, L. Baker, M. Lai, A. Bolton, et al. Mastering the game of go without human knowledge. *Nature*, 550(7676):354–359, 2017.
- [40] D. Silver, H. van Hasselt, M. Hessel, T. Schaul, A. Guez, T. Harley, G. Dulac-Arnold, D. P. Reichert, N. C. Rabinowitz, A. Barreto, and T. Degris. The predictron: End-to-end learning and planning. *International Conference on Machine Learning*, 2016. <http://arxiv.org/abs/1612.08810>.
- [41] R. S. Sutton. Dyna, an integrated architecture for learning, planning, and reacting. *SIGART Bull.*, 2(4):160–163, July 1991.
- [42] R. S. Sutton and A. G. Barto. *Reinforcement learning: An introduction*. MIT press, 2018.

- [43] E. Talvitie and S. Singh. Simple local models for complex dynamical systems. *Advances in Neural Information Processing Systems*, 21:1617–1624, 2008.
- [44] J. Tobin, R. Fong, A. Ray, J. Schneider, W. Zaremba, and P. Abbeel. Domain randomization for transferring deep neural networks from simulation to the real world. *arXiv*, abs/1703.06907, 2017. <http://arxiv.org/abs/1703.06907>.
- [45] R. van Gulick. Consciousness. In E. N. Zalta, editor, *Stanford Encyclopedia of Philosophy*. Stanford: Metaphysics Research Lab, 2004.
- [46] H. van Hasselt, A. Guez, and D. Silver. Deep reinforcement learning with double q-learning. *AAAI Conference on Artificial Intelligence*, 2015. <http://arxiv.org/abs/1509.06461>.
- [47] A. Vaswani, N. Shazeer, N. Parmar, J. Uszkoreit, L. Jones, A. N. Gomez, L. Kaiser, and I. Polosukhin. Attention is all you need. *International Conference on Neural Information Processing Systems*, 2017. <https://arxiv.org/abs/1706.03762>.
- [48] O. Vinyals, I. Babuschkin, W. M. Czarnecki, M. Mathieu, A. Dudzik, J. Chung, D. H. Choi, R. Powell, T. Ewalds, P. Georgiev, et al. Grandmaster level in StarCraft II using multi-agent reinforcement learning. *Nature*, 575(7782):350–354, 2019.
- [49] T. Wang, X. Bao, I. Clavera, J. Hoang, Y. Wen, E. Langlois, S. Zhang, G. Zhang, P. Abbeel, and J. Ba. Benchmarking model-based reinforcement learning. *arXiv*, abs/1907.02057, 2019. <http://arxiv.org/abs/1907.02057>.
- [50] T. Wang, R. Liao, J. Ba, and S. Fidler. Nervenet: Learning structured policy with graph neural networks. *International Conference on Learning Representations*, 2018.
- [51] S. M. Xie and S. Ermon. Differentiable subset sampling. *arXiv*, abs/1901.10517, 2019. <https://arxiv.org/abs/1901.10517>.
- [52] K. Xu, J. Li, M. Zhang, S. S. Du, K.-i. Kawarabayashi, and S. Jegelka. How neural networks extrapolate: From feedforward to graph neural networks. *arXiv*, abs/2009.11848, 2020. <http://arxiv.org/abs/2009.11848>.
- [53] M. Zaheer, S. Kottur, S. Ravanbakhsh, B. Póczos, R. Salakhutdinov, and A. J. Smola. Deep sets. *International Conference on Neural Information Processing Systems*, 2017. <https://arxiv.org/abs/1703.06114>.
- [54] A. Zakharov, M. Crosby, and Z. Fountas. Episodic memory for learning subjective-timescale models. *arXiv*, abs/2010.01430, 2020. <http://arxiv.org/abs/2010.01430>.

Appendices

A Architecture Details

A.1 Birdseye View of Overall Design

We present the organization of the components for the proposed CP agent in Fig 9. For the model-free baseline agent, we contributed the design of the state set encoder and the set-based value estimator. For the model-based agent, we additionally devised the design of two transition models, one with the conscious bottleneck and another without.

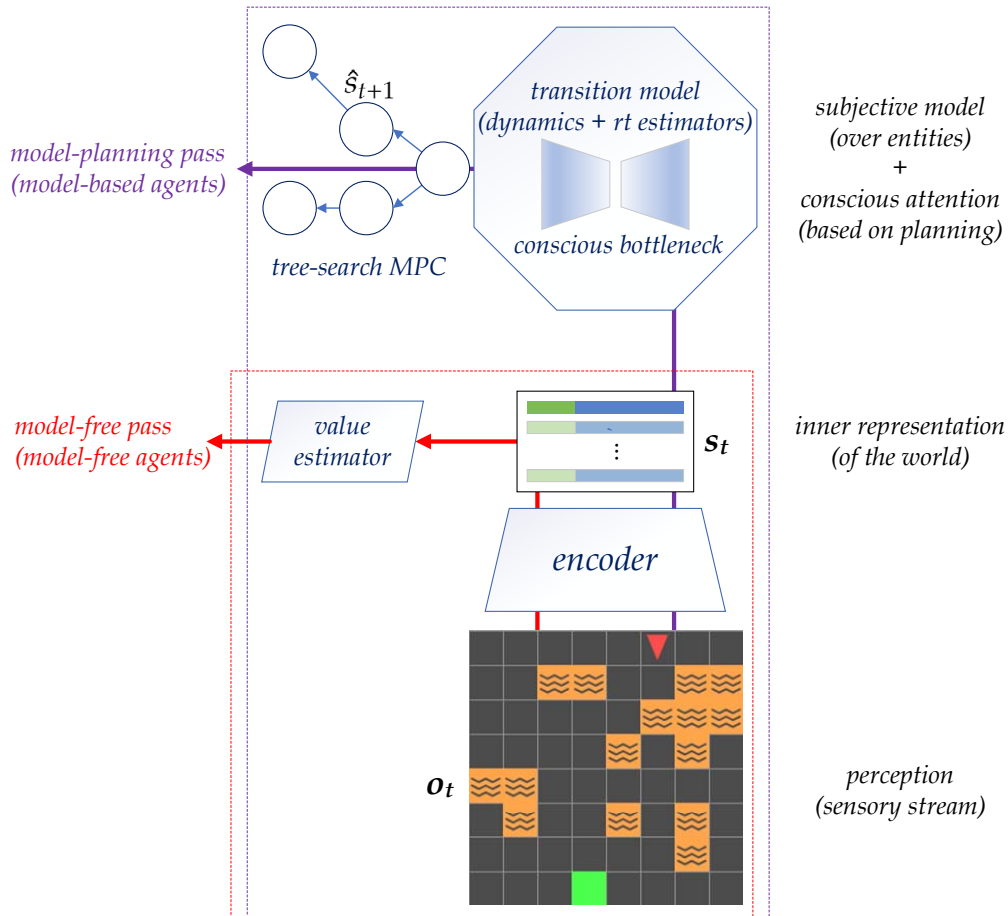


Figure 9: Overall organization of the proposed components for the CP agent. The transition model includes the reward-termination estimator, the dynamics estimator and the optionally the conscious bottleneck. Drawing similarity to the human mind, the 3-layered design corresponds naturally to human perception, inner representation and the conscious planning models.

A.2 Action-Conditioned Transformer Layer

A classical transformer layer consists of two consecutive sub-layers, the multi-head SA and the fully connected, each containing a residual pass. Similar to the processing of the positional embedding, we first embed the discrete actions into a vector and then concatenate it to every intermediate object output by the SA sub-layer. This way, each transformer layer becomes action-conditioned. An illustration of the component is provided as Figure 10.

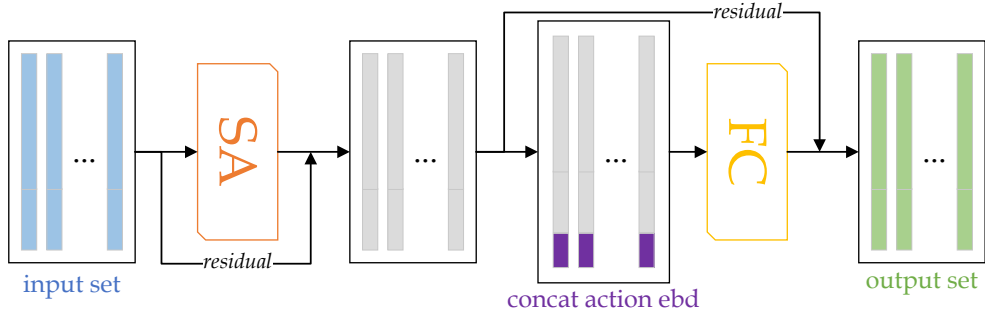


Figure 10: The computational flow of the action-conditioned transformer layer: compared to the classical transformer layers, we concatenate additionally the action embedding in the FC pass. Note that the concatenation does not happen outside the residual pass in case the dimensions do not match.

A.3 Bottleneck Selector

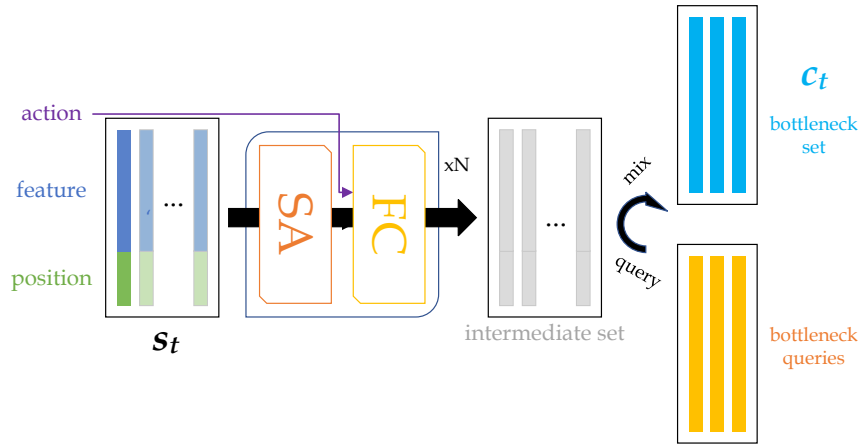


Figure 11: Design of the Bottleneck Compressor: the bottleneck set c_t is obtained by querying the whole set s_t with a learned query set of size k , using semi-hard multi-head attention. The selection is conditioned on the chosen action. Please refer to Section B.1 for more details of the query operation.

A.4 Bottleneck Integrator

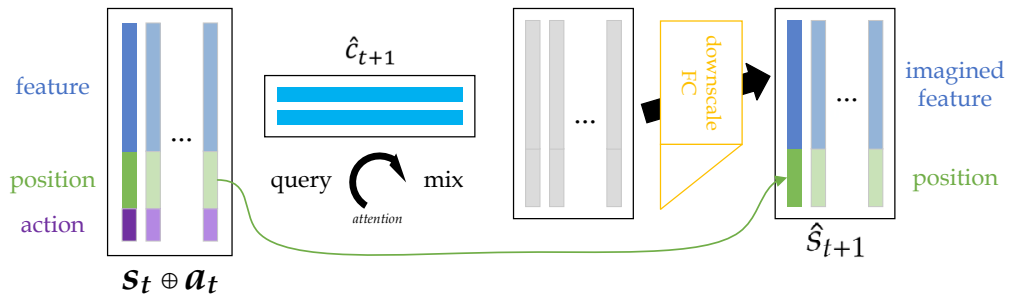


Figure 12: Design of the Bottleneck Integrator: \hat{s}_{t+1} is generated by using the action-augmented s_t to query the imagined bottleneck set \hat{c}_{t+1} . Note that there is the similar operation of downsampling objects to features and copying the positional tails. Please refer to Section B.1 for more details of the query operation.

A.5 Reward-Termination Estimator

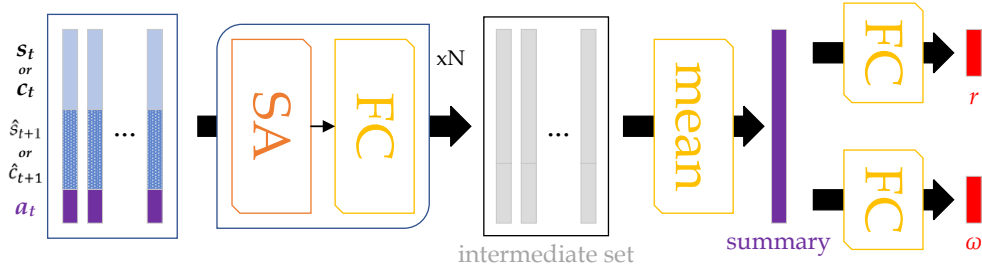


Figure 13: Design of the reward-termination estimator: the state / bottleneck set, the imagined state / bottleneck set as well as the embedding of the action are aligned and concatenated to predict the two outputs. When there is a conscious bottleneck, c_t comes from the selection, \hat{c}_{t+1} is the output of rolling c_t into the dynamics model with a_t ; When there is not, \hat{s}_{t+1} comes from the forward simulation of the model. With deterministic, it is sufficient to predict the reward and termination with only s_t and a_t . This design would also work when the dynamics simulation could handle stochastic dynamics.

In the experiments, we wanted functional architectures with minimal sizes for all the components. Thus, globally for the set-input architectures, we have limited the depth of the transformer layers to be $N = 1$ wherever possible. The FC components are MLPs with 1-hidden layer of width 64. Exceptionally, we find that the effectiveness of the value estimator needs to be guaranteed with at least 3-transformer layers. For the distributional output, while the value estimator has an output of 4 atoms, the reward estimator has only 2.

A.6 Bottleneck Dynamics

The architecture for the bottleneck dynamics (the dynamics operator that simulates \hat{c}_{t+1} from c_t, a_t) is a stack of action-conditioned transformer layers.

B Prerequisites

Here, we introduce some prerequisites for better understanding of the used operations.

B.1 Attention

One of the most important permutation invariant operations on sets of objects is the *attention querying*, which leads to the variants of attention mechanisms [5]. Here, we revisit a generic set query procedure:

For an object to *query* another set of objects, the following steps are taken:

1. The object is transformed into a query vector. In literature this is mostly done via a linear transformation.
2. The set of objects is independently transformed into two other sets of the same cardinality, named the key set and the value set, respectively.
3. The query vector now compares itself with each key vector in the key set according to some similarity function, *e.g.* scaled dot product, and obtain a vector of un-scaled “attention weights” which is later normalized into a vector with unit L_1 norm.
4. The value vectors are weighted by the normalized attention weight vector and combined (typically by linear transformations), yielding the output vector; Querying a set with another set is no different from independently applying the described procedure multiple times. The number of outputs always matches the size of the query set.

Using a set to query itself using the above procedure yield the so-called “self-attention”. Using multiple groups of linear transformations and computing the final output from the ensemble of query results is called “multi-head attention”. If we erase the lowest attention

weights and keep only the top- k ones before the L_1 re-normalization, the resulting method is called “semi-hard” attention: for the top- k matches, the attention is soft while for the bad matches, the attention is hard.

C Experiment Insights

Integer Observations For MiniGrid worlds, the observations are consisted of integers encoding the object and the status of the grids. We found that for the UP models with these integer observations, the transformer layers are not sufficiently capable to capture the dynamics. Such problem can be resolved after increasing the depth of the FC layer depth by another hidden layer. This is one of the reasons why we prioritized on using CP models for the observation-level learning of Dyna, *i.e.* CP models can handle integer features without deepening.

Similarly, we have tested the effect of increasing the depth of the linear transformations in SA layers. We did not observe significance in the enhancement of the performance, in terms of model learning or RL performance.

Addressing Memorization with Noisy Shift We discovered a generic trick to enforce better generalization based on our state-set encoding: if we use fixed integer-based positional tails which correspond to the absolute coordinates of the objects, we can add a global noise to all the x and y components in a set whenever one is encoded. By doing so, the coordinate systems would be randomly shifted every time the agent updates itself. Such shifts would render the agent unable to memorize based on absolute positions. This trick could potentially enhance the agents’ understanding of the dynamics even if in a classical static RL setting, under which the environments are fixed.

D Experiment Configurations

The source code for this work is implemented with TensorFlow 2.x and open-source at <https://github.com/PwnerHarry/CP>.

Multi-Processing: we implement a multi-process configuration similar to that of Ape-X [20], where 8 explorers collect and sends batches of 64 training transitions to the central buffer, with which the trainer trains. A pause signal is introduced when the trainer cannot consume fast enough *s.t.* the uni-process and the multi-process implementation have approximately the same performance, excluding the wall time.

Feature Extractor: We used the Bag-Of-Word (BOW) encoder suggested in [22]. Since the experiments employ a fully-observable setting, we did not use frame stack. In gym-MiniGrid-BabyAI environments, a grid is represented by three integers, and three trainable embeddings are created for the BOW representation. For each object (grid), each integer feature would be first independently transformed into embeddings, which is then mean-pooled to produce the final feature. The three embeddings are learnable and linear (with biases).

Stop criterion: Each runs stops after 2.5×10^6 agent-environment interactions.

Replay Buffer: We used prioritized replay buffer of size 10^6 , the same as in [19]. We do not use the weights on the model updates, only the TD updates.

Optimization: We have used Adam [28] with learning rate 2.5×10^{-4} and epsilon 1.5×10^{-4} . The learning rate is the same as in [31]. Our tests show that using 6.25×10^{-5} , as suggested in [19], would be too slow. The batch size is the same for both value estimator training and model training, 64. The training frequency is the same as in [19]: every 4 agent-environment interactions.

γ : Same as in [19]. 0.99.

Transformers: For the SA sublayers, we have used 8 heads globally. For the FC sublayers, we have used 2-layer MLP with 64 hidden units globally. All the transformer related components

have only 1 transformer layer except for that of the value estimator, which has 3 transformer layers before the pooling. We found that the shallower value estimators exhibit unstable training behaviors when used in the non-static settings.

Set Representation: The length of an object in the state set has length 32, where the feature is of length 24 and the positional embedding has length 8. Note that the length of objects must be dividable by the number of heads in the attentions. The positional embeddings are trainable however their initial values are constructed by the absolute xy coordinates from each corner of the gridworld ($4 \times 2 = 8$). We found that without such initialization the positional embedding would collapse.

Action Embedding: Actions are embedded as one-hot vectors with length 8.

Planning steps: for each planning session, the maximum number of simulations based on the learned transition model is 5.

Exploration: ϵ takes value from a linear schedule that decreases from 0.95 to 0.01 in the course of 10^6 agent-environment interactions, same as in [19]. For evaluation, ϵ is fixed to be 10^{-3} .

Distributional Outputs: We have used distributional outputs [7] for the reward and value estimators. 2 atoms for reward estimation (mapping the interval of $[0, 1]$) and 4 atoms for value estimation (mapping the interval of $[0, 1]$).

Regularization: We find that layer norm is crucial to guarantee the reproducibility of the performance with set-representations. We apply layer normalization [1] in the sub-layers of transformers as well as at the end of the encoder and model dynamics outputs. This applies for the NOSET baseline as well.

E More Experimental Analyses

E.1 In-Distribution Model Accuracy

We intend to demonstrate how well the bottleneck set captures the underlying dynamics of the environments. For each transition, we split the grid points into two partitions: one containing all relevant objects that changed during the transition or have an impact on reward or termination, while the other contains the remaining grid points. As a result, the dynamics error is split into into two terms which correspond to the accuracy of the model simulating the relevant and irrelevant objects respectively.

Acknowledging the differences in the norm of the learned latent representations, we use the element-wise mean of L_1 (absolute value) difference between \hat{s}_{t+1} and s_{t+1} but normalize this distance by the element-wise mean L_1 norm of s_{t+1} , as a metric of model accuracy, which we name the *relative L1*. This metric shows the degree of deviation in dynamics learning: the lower it is, the more consistent are the learned and observed dynamics.

Figure 14 (a) presents the *relative L1* error of the a CP configuration during the in-distribution learning. With the help of the bottleneck, the error for the irrelevant parts converge very quickly while the model focuses on learning the relevant changes in the dynamics. Additionally, we provide the model accuracy curves of the WM and Dyna baselines in the Appendix.

For reward and termination estimations, our results show no significant difference in estimation accuracy with different bottleneck sizes. However, they do seem to have significant impact on the dynamics learning. In Figure 14 (b), we present the convergence of the relative dynamics accuracy of different CP and UP agents. CP agents learn as fast as UP, which indicates low overhead for learning the selection and integration.

E.2 More Ablation Results

Figure 15 visualizes more experiments which highlight the effectiveness of the bottleneck’s contribution towards OOD generalization.

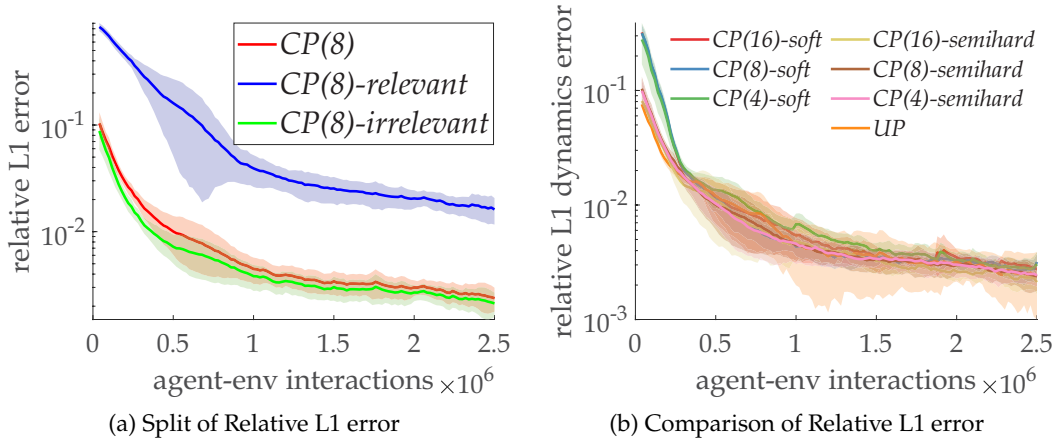


Figure 14: Curves showing in-distribution evaluation: Each band shows the mean curve (bold) and the standard deviation interval (shaded) obtained from at least 5 independent seed runs. a) Partitioning of the relative L1 dynamics prediction errors into that of the relevant objects and the irrelevant: The difference in the errors shows that the bottleneck learns to ignore the irrelevance while prioritizing on the relevant parts of the state; b) Comparison of the overall relative L1 errors (not partitioned). For CP variants, the numbers in the parentheses correspond to the bottleneck sizes and the suffixes the types of attention for the bottleneck selection. Semi-hard attention learns more quickly than soft attention at early stages but they both converge to similar accuracy levels. This is likely due to the fact that semi-hard attention is forced to pick few objects and thus to ignore irrelevant objects even at early stages of training.

E.3 Planning Steps

Intuitively we know there should be a good value for the planning step hyperparameter. If the planning steps are too few, then the planning would have little gain over model-free methods. While if the planning steps are too many, we suffer from cumulative planning errors and potentially prohibitive wall time. We tried different number of planning steps for 8-picks semi-hard CP. Note that the planning steps during training and OOD evaluation are equivalent. Such particular choice is to make sure that the planning during evaluation would be carried out to the same extent during training. The results visualized in 16 suggested that 5 planning steps achieves the best performance in OOD with difficulty 0.35.

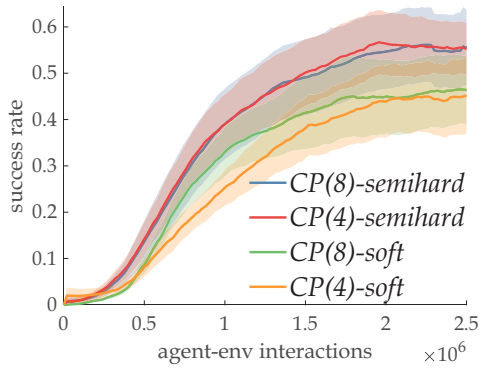
E.4 Action Regularization

We applied an additional regulatory loss that predicts the action a_t with c_t and \hat{c}_{t+1} as input, resembling the essence of an inverse model [13]. The loss is a unscaled categorical cross-entropy, like that of the termination prediction. This additional signal is shown in experiments to produce better OOD results, especially when the bottleneck is small, as visualized in Figure 17.

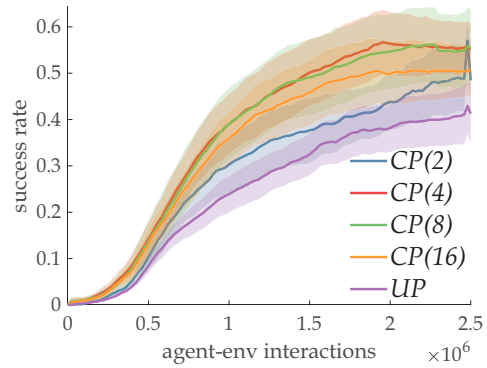
E.5 Test on Different Dynamics

To demonstrate the versatility of the proposed planning agent, we craft environments with everything else the same as before except for the dynamics: the action space is re-resigned to include 4 composite actions which first turns to some directions (forward, left, right and back based on the current facing direction) and then move forward if possible (if not stepping out of the world). Furthermore, we added randomly changing colors to every grid so that a cluttering effect is posed to hinder the agents from understanding the object interactions as well as the bottleneck selection. More specifically, the distracting colors are sampled uniformly randomly from 6 possibilities for each grid of each observation.

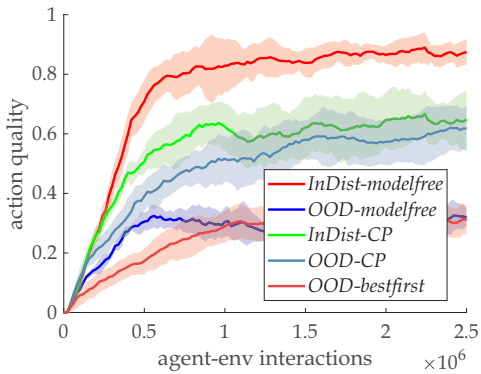
Since we have already demonstrated the superior performance of CP and UP agents over other baselines, in Figure 18, we present the learning curves of only the CP and UP agents.



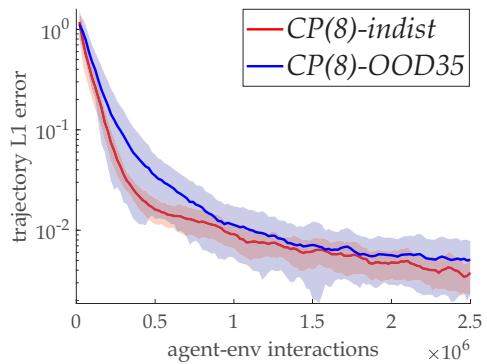
(a) Attention Type: semi-hard attention outperforms better when used in bottleneck selection



(b) Bottleneck Size: bottleneck sizes 4 and 8 perform similarly the best within $\{2, 4, 8, 16\}$. Also, the performance with bottlenecks is consistently better than that without (UP), showing the bottlenecks' effectiveness for OOD generalization



(c) Action Quality: we record if the actions taken by the methods are optimal. For in-distribution evaluation, the methods both perform well. Interestingly, the model-free agent performs superior possibly due to its simple value-based greedy policy. However in OOD evaluation, only the CP agent with the random heuristic shows neither significant deterioration nor signs of overfit in the action qualities.



(d) Tree Search Dynamics Accuracy: the curves show the cumulative L1 error of the chosen trajectory during tree search. These are obtained by comparing the imagined states simulated through multi-step planning with the help of a perfect environment model. The curves show no signs of overfit as the cumulative trajectorial dynamics accuracy during OOD evaluation is growing over time.

Figure 15: Ablation results with difficulty 0.35: each band is consisted of the mean curve and the standard deviation interval shades obtained from at least 5 independent seed runs.

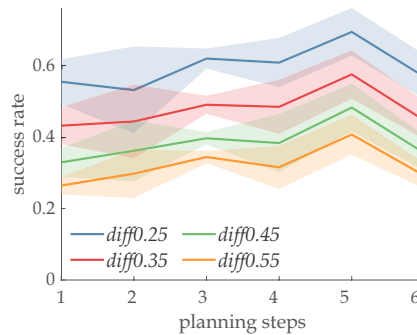


Figure 16: Success rate of CP(8) agent under OOD evaluation with difficulty 0.35. Note that for each agent variant, the planning steps used in training and OOD evaluation are the same.

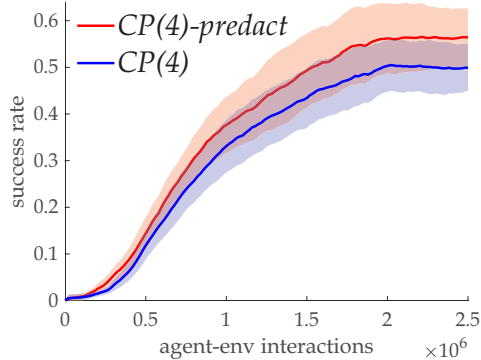


Figure 17: Impact on the success rate of CP(4) agents under OOD evaluation with difficulty 0.35 by the action regularization loss in the bottleneck. The “predact” configuration is by default enabled in the main manuscript, *i.e.* all the CP results shown except in this figure has action regularization enabled. Each point of the band correspond to the mean and standard deviation of the success rate of OOD evaluation during the last 5×10^5 M agent-environment interactions (last 20% training stage).

We observe that CP agents still perform better than the UP agent therefore re-validating the effectiveness of the bottleneck mechanism. It is likely that our state set encoder to learn to ignore the distractions and thus make the bottleneck selector to be able to direct attention to the relevant objects as what we have done for the tasks with the old dynamics.

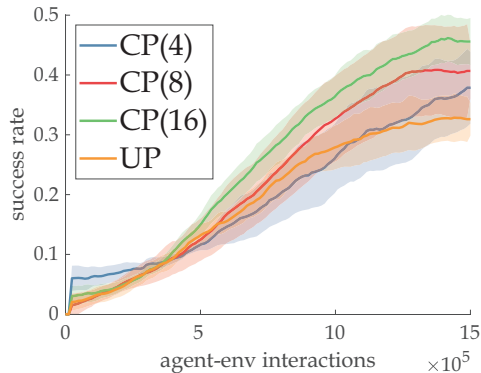


Figure 18: Performance on tasks with different dynamics: the curves are obtained from 5 independent seed runs. The composite actions shorten the length of the trajectories therefore we are using only 1.5×10^6 training steps. In this scenario, CP(16) obtains the best performance.

F Visualization of Selection

We present some visualization of the object selection during the planning steps in Figure 19. In (a), with the intention of turning left, the agent takes into the bottleneck the location of itself within the grid (visualized as the teal triangle with white surroundings, color-inverted from red-black); For (b), the agent additionally pays attention to the lava grid on its right while trying to turn right. In (a) and (b), the goal square (pink, color-inverted from green) is also paid attention but we cannot interpret such behavior. Finally in (c), we can see that the agent takes consideration into the grid (the blue lava grid, color-inverted from orange) that it is facing before taking a step-forward action. Though these visualization provides an intuitive understanding to the agents’ behavior, they do not serve statistical purposes.

We additionally have collected the coverage ratio of all the relevant objects by the selection phase in all the in-distribution and OOD evaluation cases along the process of learning. The collected data on bottleneck sizes 4, 8 and 16 indicate that the coverage is almost perfect very early on during training. We do not provide these curves because the convergence to 100%

is so fast that the curves would all coincide with line $y = 1$, with some minor fluctuations of the standard deviation shades.

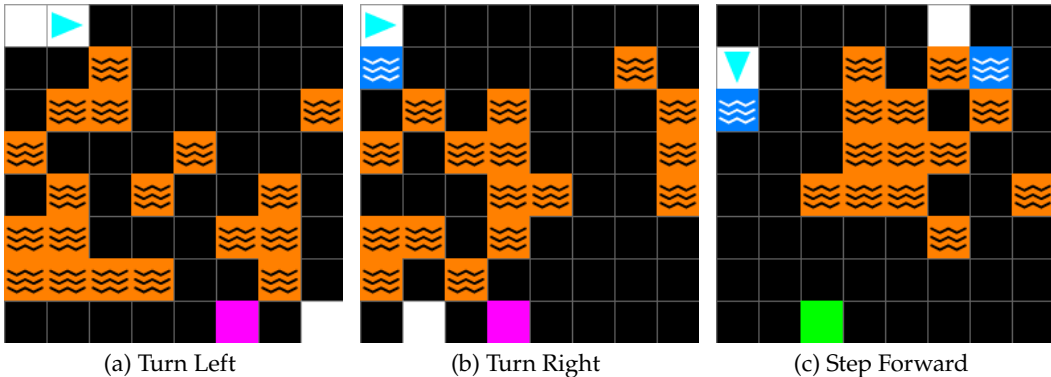


Figure 19: Visualization of the bottleneck selection given the observation and specific actions. These figures are extracted from a fully trained CP(2) agent under OOD evaluation. The bottleneck is set to very small for clearer visualization purposes. We invert the color of the selected objects by the best performing head, *i.e.* the head that covers the most relevant objects, though the selection quality would be sufficiently justified if *all* the heads could *cumulatively* cover all the interested objects. The grids of the selection would be at least 2 but at most 4 due to the design.

G Details of Compared Baseline Methods

G.1 Staged Training (World Models)

The agents with World Model (WM) trained in stages share the same architectures as their CP or UP counterparts. The main difference is that the WM agents adopt a 2-staged training strategy: In the first 10^6 agent-environment interactions, only the model is trained and therefore the representation is only shaped by the model learning. In the first stage the agent relies on a uniformly random policy. After 10^6 interactions, the agent freezes its encoder as well as the model to carry out value estimator learning. Note that the agent carries out tree-search MPC with the frozen model in the second stage. Compared to CP or UP, the exploration scheme is delayed but unchanged. Also, the training configurations do not change.

G.2 Dyna

The Dyna agents share the model-free part of the architecture as CP or UP. The models that Dyna baselines learn are powered by our action-conditioned set-to-set architecture on an observation-level. The training timings for both the model and the value estimator are not changed, though they do not jointly shape the representation and are used very differently compared to CP or UP. In our implementation, the generation of imagined transitions is carried out by dedicated processes. These processes generate transitions and send them to a dedicated global replay buffer of size 1024. The small size is to ensure that the delusional transitions would be washed out soon after the model is effective. The TD learning of the value estimator samples a double-sized mini-batch, half from the buffer of real transitions and half imagined. While the model training uses only the true transitions, with unit-sized batches. Since our model is not generative, we rely on free-of-budget model-free agents to collect true $\langle s, a \rangle$ pairs from the environment and then complete the missing parts of the transitions (reward, termination and next observation) using the model (for the Dyna baseline with true dynamics, we just collect the whole transition exclude the model). This way, the transitions would follow the state-action occupancy jointly defined by the MDP dynamics and the policy. The approach is a compromise to implement a correctly performing Dyna agent with a non-generative model.

G.3 NOSET

The NOSET baseline embraces traditional vectorized representations. We use the same encoder but instead of transforming the feature map into a set, we flatten it and the linearly project it to some specific dimensionality (256). This vector would be treated as s_t , the same as the most existing DRL practices. Since all set-based operations would be now obsolete for the vectorized representation, they are substituted with 3-layered FCs with hidden width 512. The 2-layered dynamics model employ a residual connection with the expectation that the model might learn incremental changes in the dynamics. In our experiments with randomly generated environments for each episode, the NOSET baseline performs miserably. However, if we instead randomly generate an environment at the start of the run and use the same one for the whole run, *i.e.* adopt the more classical RL setting, we find that the NOSET baseline is able to perform effectively, as shown in Figure 20.

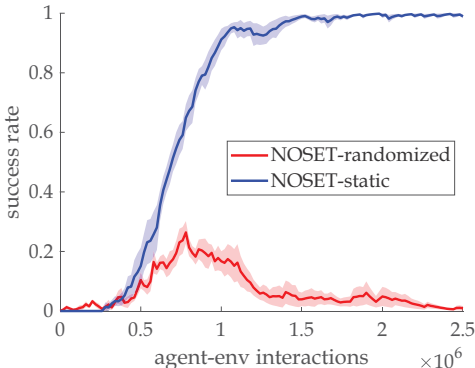


Figure 20: NOSET baseline performance on randomized and static random environments. Each band is consisted of the mean curve and the standard deviation interval shades obtained from at least 5 independent seed runs.

The dimension of the state representation, the widths and the depths of the FC layers are obtained through coarse grid tuning of the exponents of 2. We find that architectures exceeding the chosen size are hardly superior in terms of performance.

H Tree Search MPC

The agent (re-)plans at every timestep using the learned model in the hidden state level. The in-distribution planning strategy is a best-first search MPC heuristic. While the OOD planning heuristic is random search. Note that no matter which heuristic is used, the chosen action is always backtracked by the trajectory with the most return.

We present the pseudocode of the tree search MPC in Algorithm 1. Additionally, we provide an example showing how the best-first heuristic works in an assumed decision time with $\gamma = 1$ and $|\mathcal{A}| = 3$ and maximum planning steps 3.

I Failed Experiments

We list here some of our failed trials along our way of exploring the topic of this work.

I.1 Straight-Through Hard Subset Selection with Gumbel

We initially tried to use Gumbel subset selection [51] to implement a hard selection based bottleneck but to no avail. We expect the model to pick the right objects by generating a binary mask and then use the masked objects as the bottleneck set. This two-staged design would align more with the consciousness theories and would yield clearer interpretability. However, it suffers from an implicit chicken-and-egg problem that we have not successfully addressed: to learn how to pick, the model should understand the dynamics. Yet if the

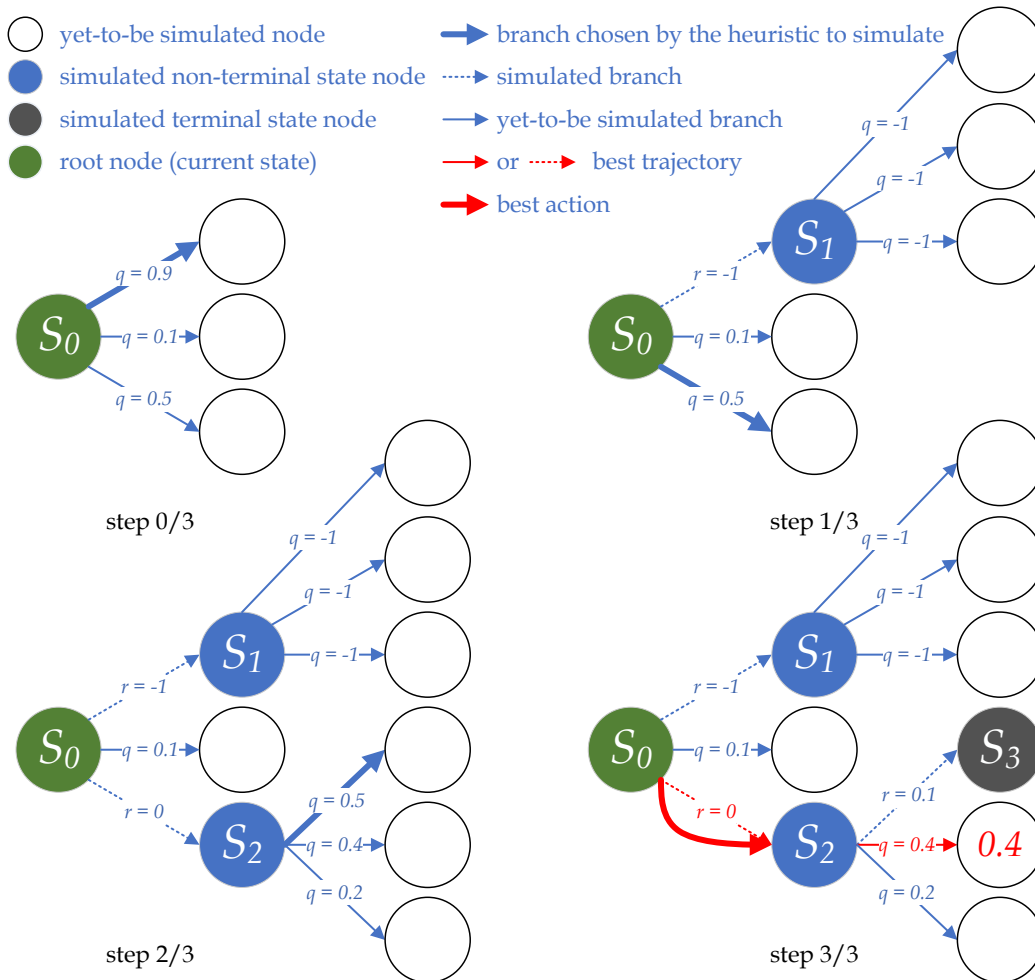


Figure 21: Example of the Best-First Heuristic: Step 0 / 3) Start of planning, with the root node and three branches. The branch $\langle s_0, a_0 \rangle$ is chosen due to the best-first heuristic. If we employ the random search heuristic, like what we do in OOD evaluation, a random branch would be chosen; Step 1 / 3) We expand the chosen branch, popped out of the priority queue. A new node is constructed, together with its out-reaching branches, which are added to the queue. Now the queue has 5 branches in it. The heuristic marks $\langle s_0, a_2 \rangle$ to be the next simulated branch; Step 2 / 3) Simulation of $\langle s_0, a_2 \rangle$ is finished and $\langle s_2, a_0 \rangle$ is marked; Step 3 / 3) Node S_3 is imagined via $\langle s_2, a_0 \rangle$ but it is estimated to be a terminal state. Now, the tree search budget is depleted. We locate the root node branch $\langle s_0, a_2 \rangle$ which leads to the trajectory with the most promising return 0.4.

Algorithm 1: Prioritized Tree-Search MPC

Input: s_0 (current state), \mathcal{A} (action set), \mathcal{M} (model), Q (value estimator), γ (discount)
Output: a^* (action to be taken)

```
 $q = \text{queue}(); q_T = \text{queue()} // q_T \text{ for terminal nodes}$  $n_u = \text{NODE}(s_0, \text{root} = \text{True}) // n_u \text{ denotes a node with branches unprocessed nor in } q$ while  $\text{True}$  do  
  if  $n_u.\omega$  then  
     $q_T.\text{add}(\langle n_u, n_u.\sigma \rangle) // \text{identified as a terminal state. } n_u \text{ is added to } q_T \text{ using}$   
      bisection, together with the discounted sum of the simulated rewards along the  
      way  $n_u.\sigma$   
  else  
    for  $a \in \mathcal{A}$  do  $q.\text{add}(\langle n_u, a, n_u.\sigma + \gamma^{n_u.\text{depth}} \cdot Q(n_u.s, a) \rangle) // \text{bisect w.r.t. priority};$   
  if  $\text{isempty}(q)$  then break // tree depleted;  
   $n_c, a_c, v_e = q.\text{pop}() // \text{get branch with highest priority; for in-distribution setting,}$   
    priority is the estimated value of the leaf trajectory  
  if budget depleted then break // termination criterion met;  
   $\hat{s}, \hat{r}, \hat{\omega} = \mathcal{M}(n_c.s, a_c) // \text{simulate the chosen branch}$   
   $n_u = \text{NODE}(\hat{s}, \text{parent} = n_c)$   
  if  $n_c.\text{depth} > 0$  then  $n_u.a_b = n_c.a_b$ ; else  $n_u.a_b = a_c // \text{descendants trace root action};$   
   $n_u.\omega = \hat{\omega}; n_u.\sigma = n_c.\sigma + \gamma^{n_c.\text{depth}} \cdot \hat{r}$   
 $n_c, a_c, v_e = q.\text{pop}(\text{'highest value'}) // \text{get branch with highest value within the}$   
  expandables  
   $n^* = n_c;$   
  if  $\neg \text{isempty}(q_T)$  then  
     $n_T = q_T.\text{pop}(\text{'highest value'}) // \text{get node with highest value within simulated}$   
      terminal states  
    if  $n_T.\text{value} \geq v_e \vee \text{isempty}(q)$  then  $n^* = n_T;$   
if  $\text{isroot}(n^*)$  then  $a^* = a_c$ ; else  $a^* = n^*.a_b;$ 
```

model does not pick the right objects frequently enough, the dynamics would never be understood. Our proposed semihard / soft approaches address such problem by essentially making the two staged selection and simulation as a whole for the optimization.

J More Discussions on Limitations & Future Directions

This paper serves as a proof-of-concept of an interesting research direction: System-2 DRL. It is healthy to point out the limitations of this work as well as some interesting future research directions:

- This paper does not solve the “planning horizon dilemma”, a fundamental issue of error accumulation of tree search expansion using imperfect models [25, 24, 49]. We strongly believe that incorporating temporal abstraction of actions, e.g. options or subjective time models [54] would gracefully address such problem. Promising as this is, introducing temporal abstraction to model-based RL is non-trivial and requires considerate investigation.
- Constant replanning may be prohibitive in reaction-demanding environments, especially when equipped with a computationally expensive set-based transition model. A planning strategy could be devised to control when or where for the agent to carry out planning, through the means of capturing uncertainty.
- The CP model cannot yet learn stochastic dynamics. The difficulty lies in the design of a compatible end-to-end trainable set-to-set machinery. We would like to address this in future.